Results in Physics 14 (2019) 102396

Contents lists available at ScienceDirect

Results in Physics

journal homepage: www.elsevier.com/locate/rinp

Supercontinuum generation in the absence and in the presence of color centers in NaCl and KBr

A. Marcinkevičiūtė, V. Jukna, R. Šuminas, N. Garejev, G. Tamošauskas, A. Dubietis*

Laser Research Center, Vilnius University, Saulėtekio Avenue 10, LT-10223 Vilnius, Lithuania

ABSTRACT

We study supercontinuum generation with femtosecond mid-infrared laser pulses in NaCl and KBr crystals when pumped at the vicinity of their zero group velocity dispersion points. Almost three octave-spanning SC spectra (covering the 0.7–5.4 μm and 0.85–5.4 μm ranges in 5 mm-thick NaCl and KBr samples, respectively) were produced by filamentation of 70 fs, 3.6 μm input pulses in continuously translated samples. In the static setup, we show that rapid formation of persistent color centers (within a few seconds at 500 Hz repetition rate) inside these materials results in a marked decrease (by 40%) of the overall energy transmittance and in significant narrowing of SC spectra. We also demonstrate that the effect of color centers on the SC spectrum could be adequately simulated numerically using a simple phenomenological model which considers color centers as impurities with a certain energy bandgap.

Introduction

Supercontinuum (SC) generation through filamentation of femtosecond laser pulses in bulk solid-state media represents a simple, efficient and well-established technique for the production of coherent broadband radiation at various parts of the optical spectrum [1]. SC generation in the mid-infrared spectral range currently attracts a great deal of scientific and technological interest. This interest is inspired by the time-resolved spectroscopy in the molecular fingerprint region and in particular, by the applications in the emerging field of ultrafast mid-infrared nonlinear optics, offering an easy way for production of few optical cycle pulses, which could be further shaped and/or parametrically amplified up to very high peak powers, see e.g. [2,3]. To date, the ultrabroad, multioctave SC spectra spanning the wavelengths from the UV to the MIR have been produced with mid-infrared pumping in a number of popular wide-bandgap dielectric materials: oxides, such as YAG, sapphire and fused silica, and alkali metal fluorides, such as CaF_2, BaF_2 and LiF [4–10].

Proper choice of the nonlinear medium is an important issue concerning the generation of broadband radiation within a desired wavelength range, as the physical factors that define the width of the SC spectrum are tightly linked to relevant optical parameters of the material. It is well established that the order of the multiphoton absorption (that is the ratio of the material bandgap and the incident photon energy) [11] and chromatic dispersion [12] define the attainable blue-shift of the SC spectrum in a given nonlinear material. On the other hand, an explicit numerical study of SC generation in various nonlinear materials with mid-infrared laser pulses suggested that the zero GVD wavelength may serve as a reasonably good indicator for attainable red-shift of the SC spectrum [13].

For what concerns the latter criterion, the zero GVD points of the above mentioned materials are located in the near infrared, at wavelengths generally shorter that 2 μm. Therefore, the materials whose zero GVD points are located in the MIR, e.g. soft glasses [14–17], semiconductors [18–23] and narrow bandgap dielectric crystals [24,25] emerge as very efficient nonlinear media for SC generation in the mid-infrared. In further search of other suitable materials, the numerical simulations of filamentation and spectral broadening in alkali halide crystals identified them as attractive candidates. To this end, the simulations with pump pulses having carrier wavelengths slightly above their zero GVD points, predict that multioctave SC spectra with very large red shifts reaching into the far-infrared could be potentially achieved [13].

In this paper we report on filamentation and multioctave SC generation in sodium chloride (NaCl) and potassium bromide (KBr) crystals using 70 fs pulses with a carrier wavelength of 3.6 μm, which falls slightly above the zero GVD point of NaCl and slightly below that of KBr. We demonstrate that these alkali metal halide crystals produce multioctave SC in the infrared, however they are prone to color center formation, which markedly modifies the shape and the width of the SC spectra.

Materials and methods

The experimental setup is depicted in Fig. 1. The mid-infrared input pulses with a central wavelength of 3.6 μm and 70 fs duration at 500 Hz

* Corresponding author.
E-mail address: audrius.dubietis@ff.vu.lt (A. Dubietis).

https://doi.org/10.1016/j.rinp.2019.102396
Received 30 April 2019; Received in revised form 27 May 2019; Accepted 27 May 2019
Available online 31 May 2019

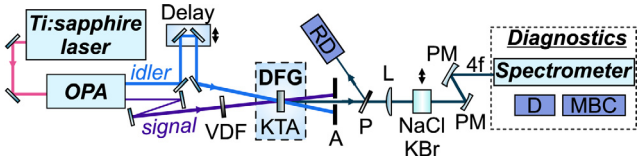

Fig. 1. Schematic of the experimental setup. OPA: optical parametric amplifier, DFG: difference frequency generation, NaCl, KBr: crystal samples; arrows indicate the direction of translation, DM: dichroic mirror, PM: parabolic mirrors, VDF: variable density filter, L: focusing lens, MBC: micro-bolometric camera, A: iris aperture, P: thin YAG plate, RD: reference detector.

repetition rate were produced by the difference frequency generation (DFG) between the signal (1309 nm) and idler (2057 nm) outputs of the Ti:sapphire laser-pumped optical parametric amplifier OPA (Topas-Prime, Light Conversion Ltd.) in a 1 mm-thick KTA crystal. DFG was performed in a slightly non-collinear geometry (the external beam crossing angle 0.3°), to easily remove the residual signal and idler components. The mid-infrared beam was focused with a BaF_2 lens L ($f = +100$ mm) into the focal spot of 55 μm FWHM diameter located 2 mm inside the nonlinear medium. The input pulse energy was varied by adjusting the energy of the signal wave by means of a neutral metal-coated variable density filter VDF (NDL-25C-2, Thorlabs Inc.) and was set to produce a single filament at the output of the nonlinear medium. This was verified by monitoring the near-field intensity profile of the output beam with a micro-bolometric camera MBC (WinCamD, FIR2-16-HR). The spectral measurements were performed using a home-built scanning prism spectrometer with Si and InAsSb detectors, providing an effective detection range of 0.2–5.8 μm. In these measurements, the output face of the nonlinear medium was imaged by means of Ag-coated parabolic mirrors (PM) onto the input slit of the spectrometer, so effectively coupling the axial portion of the SC radiation along with a fraction of conical emission. The energy measurements were performed with a pyroelectric detector (D).

The nonlinear media used were uncoated NaCl and KBr samples of 5 mm thickness. The relevant optical parameters of these materials are presented in Table 1. NaCl and KBr are crystals with cubic symmetry and exhibit remarkable transparency ranges from the UV to the far-infrared and relatively large nonlinear indexes of refraction. The chosen pump wavelength of 3.6 μm falls close to their zero GVD points: in NaCl, GVD is slightly anomalous ($g = -34$ fs^2/mm), while in KBr, GVD is slightly normal ($g = +5$ fs^2/mm).

Results

Ultrabroadband, multi-octave SC spectra were recorded in NaCl and KBr samples of 5 mm thickness, pumped by 70 fs, 3.6 μm pulses having energies of 3.56 and 2.23 μJ, respectively, after accounting for a Fresnel reflection from the input faces of the samples, and illustrated in Fig. 2. These input pulse energies convert to the input powers of 51 MW and 32 MW, which correspond to 1.7 P_{cr} and 2.0 P_{cr} in NaCl and KBr,

Table 1
Relevant linear and nonlinear optical parameters of NaCl and KBr. U_g is the bandgap, n_0 and g are the linear refractive index and the GVD coefficient at 3.6 μm, respectively, λ_0 is the zero GVD wavelength calculated from the dispersion equations given in [26]. n_2 is the nonlinear refractive index; data from [27,28].

Material	NaCl	KBr
Transmittance (μm)	0.17–18	0.2–30.6
U_g (eV)	9.0	7.6
n_0	1.523	1.536
n_2 (× 10^{-16} cm^2/W)	4.35	7.95
λ_0 (μm)	2.76	3.83
g (fs^2/mm)	− 34	+ 5

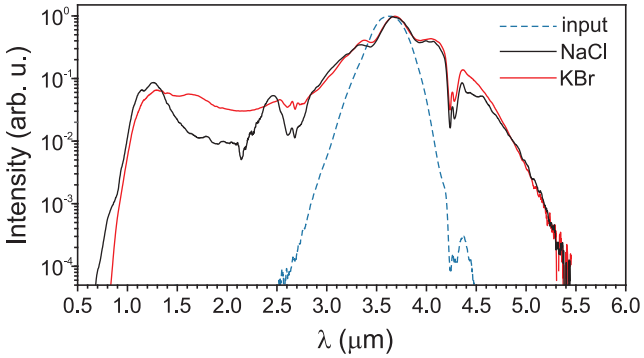

Fig. 2. Supercontinuum spectra in NaCl (black curve) and KBr (red curve) produced by filamentation of 70 fs, 3.6 μm pulses and recorded while continuously translating the samples. The input pulse energies were 3.56 and 2.23 μJ, respectively. The input pulse spectrum is shown by a dashed curve. (For interpretation of the references to colour in this figure legend, the reader is referred to the web version of this article.)

respectively, where $P_{cr} = 3.77\lambda^2/8\pi n_0 n_2$ is the critical power for self-focusing calculated from the data provided in Table 1. During spectral scan, the samples were continuously translated (perpendicular to the pump beam direction) to avoid the influence of color center formation. More specifically, the measured SC spectrum in NaCl covered the wavelength range from 700 nm to 5.4 μm (at the 10^{-4} intensity level) that corresponds to 2.9 optical octaves. A slightly narrower SC spectrum, in the 0.85–5.4 μm range, corresponding to 2.7 optical octaves was measured in KBr. Note distinct spectral dips around 2.7 and 4.25 μm that are absorption signatures of atmospheric H_2O and CO_2, respectively. Signatures of H_2O and CO_2 absorption could be removed in, e.g., nitrogen atmosphere, which also would be useful for extending the longevity of uncoated NaCl and KBr crystals, and especially their surfaces that degrade with time due to interaction with atmospheric humidity. These spectra further serve as references for monitoring spectral modifications due to evolving color centers in these materials when SC was generated in a static setup.

Indeed, it is well known that most of alkali metal halide crystals are prone to formation of color centers that affect the SC spectrum to a certain degree, as experimentally demonstrated in LiF [8,29–32] and to some extent, in PbF_2[25]. In alkali halides, color centers are products of self-trapped exciton decay, and the mechanism of their formation is known fairly well. After nonlinear ionization through multiphoton absorption that generates electrons and holes, the process starts from exciton creation, that is followed by self-trapping of the exciton and ends up with its decay, resulting in an occurrence of color centers [33]. The color centers are associated with electron trapping at a halide vacancy (F centers) and two F centers on adjacent sites (M centers, or the so-called F_2 centers) [34]. Color centers are responsible for the occurrence of broad absorption bands, whose peak wavelengths are located in the visible (F centers) and near infrared (M centers). More specifically, broad absorption bands in NaCl are centered at 460 nm (F centers) and at 725 nm (M centers) [35], while in KBr the respective absorption bands associated with F and M centers are more red-shifted and peak at 625 nm and 930 nm, respectively [36]. In addition to these, ultraviolet absorption bands are observed as well, that are due to V centers associated mostly with hole traps by impurities in these materials. The process of color center formation in NaCl and KBr crystals is very fast, taking place on a μs time scale, as demonstrated in the conditions of intense femtosecond UV irradiation by pump-probe measurements [35,36]. Rapid accumulation of color centers was justified by a drop of transmission at selected probe wavelengths, that eventually saturates after a few seconds at 1 kHz repetition rate [34].

Fig. 3(a) shows the evolution of SC spectrum in NaCl as a function of exposure time. Due to color center formation, the SC spectrum experiences a considerable shrinking along with a decrease of the spectral

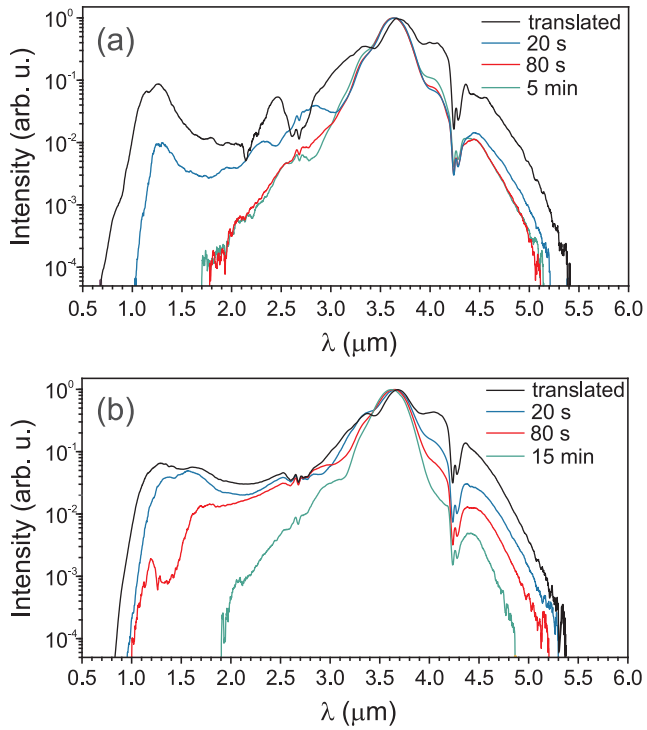

Fig. 3. Evolutions of SC spectra in (a) NaCl, (b) KBr as functions of exposure time.

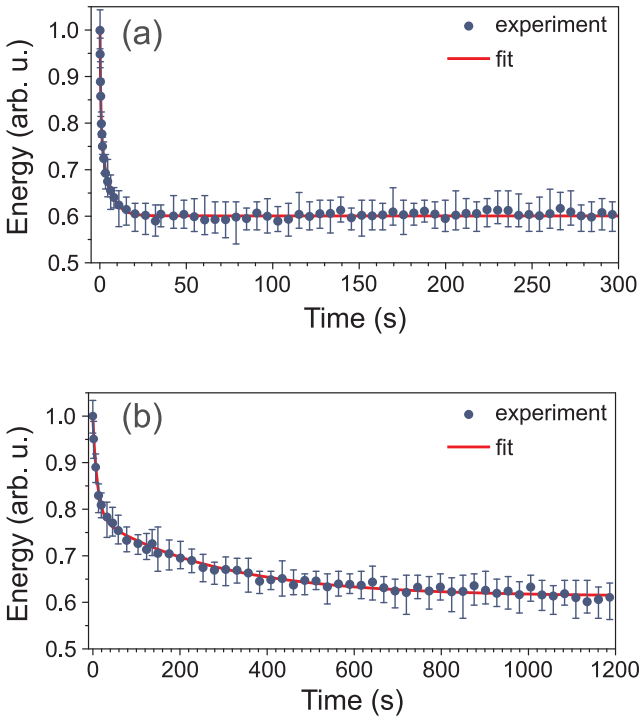

Fig. 4. Measured energy transmittances (full circles) and their two-exponential fits (solid curves) for (a) NaCl and (b) KBr samples in a static setup. The plots are normalized to the sample transmittances in the absence of color centers. Each data point represents an average over 25 laser shots (the time interval of 50 ms) and for better data readability, only every third data point is displayed.

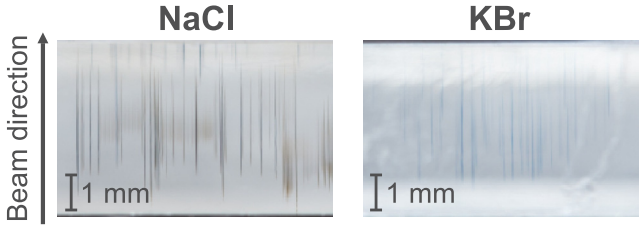

Fig. 5. Photographs of (a) NaCl and (b) KBr samples with filament-induced color centers, which were produced by slightly varying the input pulse energies (around the specified values for NaCl and KBr) and exposure times (from a few tens of seconds to a few tens of minutes). (For interpretation of the references to colour in this figure legend, the reader is referred to the web version of this article.)

intensity on both sides of the carrier wavelength, and spectral shrinking is particularly pronounced at the short-wavelength side. Note that dramatic spectral changes emerge very quickly (within a few tens of seconds at 500 Hz repetition rate). Thereafter color center-induced spectral dynamics settle down after 80 s of exposure, and the SC spectrum keeps its new shape with a markedly reduced width (1.8–5.1 μm, as defined at the 10^{-4} intensity level) for the rest of the measurement time. A similar color center-induced narrowing of the SC spectrum was observed in KBr, as illustrated in Fig. 3(b). However, in the present case, the spectral dynamics are markedly slower: the shrinking of the SC spectrum finally settles just after 15 min of exposure time.

Changes of the SC spectra correlate very well with decrease of energy transmittances, recorded for both material samples and shown in Fig. 4. Here the energy transmittances are normalized to the transmittance levels which were measured in the absence of color centers, i.e. by continuously translating the samples. In other words, the unity transmittance was set with an account for Fresnel reflection from the output face of the sample and energy losses that occur in the filamentation process that are contributed by multiphoton absorption and absorption of free electron plasma via inverse Bremsstrahlung effect. Therefore the illustrated energy losses are contributed solely by linear and nonlinear absorption of the color centers. Notice that the energy transmittance decreases very rapidly and color centers take an immediate effect on the SC spectral width.

NaCl shows a prompt drop of energy transmittance that is well fitted by two exponents with time constants of 0.53 s and 5.1 s, as shown in Fig. 4 (a). The energy transmittance after 20 s settles down to 60% of the initial transmittance value, which thereafter remains constant for the rest of the measurement. The energy transmittance of KBr sample settles to an almost identical final value, however, the process is more extended in time (two-exponential decay with time constants of 10.6 s and 282 s), see Fig. 4(b). An established two-exponential decay in both materials could be attributed to different speeds of formation of F (a faster exponent) and M (a slower exponent) centers.

Finally, residual color centers are easily seen by a naked eye, as illustrated in Fig. 5. Their specific colors: moss-green in NaCl and ink-blue in KBr, are due to F center absorption bands in the visible range. Note that color centers are formed only at the filament site, i.e., where intensity and nonlinear losses due to multiphoton and free electron absorption are the highest, enabling to trace precisely the filament path.

The SC spectra in NaCl were simulated numerically using a model which solves a unidirectional nonparaxial propagation equation for the pulse envelope, see [37,38] for details, taking relevant material parameters from Table 1 and input pulse parameters from the experiment. The effect of color centers was accounted for using a phenomenological approach, which considers them as evenly distributed impurities with an energy bandgap of 2.7 eV that corresponds to the strongest absorption band centered at 460 nm due to F centers [35]. The numerically simulated SC spectra using different impurity concentrations, which could be directly associated with accumulation of color centers while increasing exposure time in the experiment, are presented in Fig. 6.

The numerical results demonstrate a marked narrowing of SC spectrum as the density of the impurities increases. Of course, inclusion

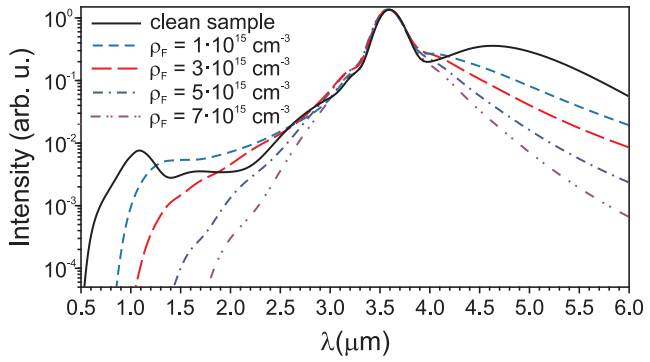

Fig. 6. Numerically simulated SC spectra in NaCl with different impurity densities ρ_F that mimic the effect of color center absorption. (For interpretation of the references to colour in this figure legend, the reader is referred to the web version of this article.)

of color centers in the numerical model in that way, is a very simple approximation, since color center-induced modifications of relevant material properties, e.g., linear and nonlinear refractive indexes and dispersion were not considered. Nevertheless, even this simple numerical approach gives a fair agreement with experimentally recorded spectral dynamics. Therefore the following qualitative mechanism how color centers act on the width of SC spectrum could be unveiled. Since the absorption band of color centers (F-centers, in the present case) does not overlap with SC spectrum, they do not absorb the SC radiation directly. This suggests that color centers absorb the input pulse energy via multiphoton absorption. The observed shrinking of SC spectrum is then explained by reduction of the effective material bandgap through formation of color center absorption band, which results in a decrease of clamping intensity and thus an increase of the limiting filament diameter, which in turn yields a narrower SC spectrum [11]. Multiphoton absorption of color centers readily produces a larger number of free electrons, which are then accelerated via inverse Bremsstrahlung and avalanche, and thus participate in further production of color centers. This lasts until the process reaches a certain equilibrium between the production and annihilation of color centers.

Conclusions

In conclusion, we experimentally studied SC generation in NaCl and KBr samples pumped by femtosecond mid-infrared laser pulses, in the absence and in the presence of color centers. Almost three octave-spanning SC spectra were recorded in these materials in the absence of color centers, as the samples were continuously translated during the measurement. In contrast, in the static setup, color centers in both materials are produced very quickly, resulting in a considerable reduction of the SC spectral widths and energy transmittances. The narrowing of SC spectrum in NaCl was simulated numerically using a simple phenomenological model of color centers, which considers them as impurities with an energy bandgap of 2.7 eV that corresponds to the F-center absorption band centered at 460 nm.

These results suggest that alkali metal halide crystals, such as NaCl and KBr may serve as potentially attractive nonlinear materials for multi-octave SC generation in the mid-infrared, however, a special care has to be taken to reduce the effect of color centers, which evolve on a very fast time scale (the estimated energy decay rates were few seconds at 500 Hz repetition rate). In particular, these effects should be taken into account considering the nonlinear propagation of very high power laser pulses with carrier wavelengths in the mid-infrared, where e.g., NaCl is considered as an attractive material for self-compression due to suitable nonlinear and dispersive properties [39].

Acknowledgment

The authors acknowledge financial support from the European Regional Development Fund (ERDF), Grant No. 1.2.2-LMT-K-718-02-0017.

References

[1] Dubietis A, Tamošauskas G, Šuminas R, Jukna V, Couairon A. Ultrafast supercontinuum generation in bulk condensed media. Lith J Phys 2017;57:113–57.
[2] Pires H, Baudisch M, Sanchez D, Hemmer M, Biegert J. Ultrashort pulse generation in the mid-IR. Prog Quantum Electron 2015;43:1–30.
[3] Krogen P, Suchowski H, Liang H, Flemens N, Hong KH, Kärtner FX, Moses J. Generation and multi-octave shaping of mid-infrared intense single-cycle pulses. Nat Photon 2017;11:222–6.
[4] Silva F, Austin DR, Thai A, Baudisch M, Hemmer M, Faccio D, Couairon A, Biegert J. Multi-octave supercontinuum generation from mid-infrared filamentation in a bulk crystal. Nature Commun 2012;3:807.
[5] Darginavičius J, Majus D, Jukna V, Garejev N, Valiulis G, Couairon A, Dubietis A. Ultrabroadband supercontinuum and third-harmonic generation in bulk solids with two optical-cycle carrier-envelope phase-stable pulses at 2 μm. Opt Express 2013;21:25210–20.
[6] Dharmadhikari JA, Deshpande RA, Nath A, Dota K, Mathur D, Dharmadhikari AK. Effect of group velocity dispersion on supercontinuum generation and filamentation in transparent solids. Appl Phys B 2014;117:471–9.
[7] Liang H, Krogen P, Grynko R, Novak O, Chang CL, Stein GJ, Weerawarne D, Shim B, Kärtner FX, Hong KH. Three-octave-spanning supercontinuum generation and sub-two-cycle self-compression of mid-infrared filaments in dielectrics. Opt Lett 2015;40:1069–72.
[8] Garejev N, Tamošauskas G, Dubietis A. Comparative study of multioctave supercontinuum generation in fused silica, YAG, and LiF in the range of anomalous group velocity dispersion. J Opt Soc Am B 2017;34:88–94.
[9] Marcinkevičiūtė A, Garejev N, Šuminas R, Tamošauskas G, Dubietis A. A compact, self-compression-based sub-3 optical cycle source in the 3–4 μm spectral range. J Opt 2017;19:105505.
[10] Chekalin SV, Dormidonov AE, Kompanets VO, Zaloznaya ED, Kandidov VP. Light bullet supercontinuum. J Opt Soc Am B 2019;36:A43–53.
[11] Brodeur A, Chin SL. Band-gap dependence of the ultrafast white-light continuum. Phys Rev Lett 1998;80:4406–9.
[12] Kolesik M, Katona G, Moloney JV, Wright EM. Physical factors limiting the spectral extent and band gap dependence of supercontinuum generation. Phys Rev Lett 2003;91:043905.
[13] Frolov SA, Trunov VI, Leshchenko VE, Pestryakov EV. Multi-octave supercontinuum generation with IR radiation filamentation in transparent solid-state media. Appl Phys B 2016;122:124.
[14] Liao M, Gao W, Cheng T, Duan Z, Xue X, Kawashima H, Suzuki T, Ohishi Y. Ultrabroad supercontinuum generation through filamentation in tellurite glass. Laser Phys Lett 2013;10:036002.
[15] Yu Y, Gai X, Wang T, Ma P, Wang R, Yang Z, Choi DY, Madden S, Luther-Davies B. Mid-infrared supercontinuum generation in chalcogenides. Opt Mater Express 2013;3:1075–86.
[16] Mouawad O, Béjot P, Billard F, Mathey P, Kibler B, Désévédavy F, Gadret G, Jules JC, Faucher O, Smektala F. Mid-infrared filamentation-induced supercontinuum in As-S and an As-free Ge-S counterpart chalcogenide glasses. Appl Phys B 2015;121:433–8.
[17] Stingel AM, Vanselous H, Petersen PB. Covering the vibrational spectrum with microjoule mid-infrared supercontinuum pulses in nonlinear optical applications. J Opt Soc Am B 2017;34:1163–8.
[18] Lanin AA, Voronin AA, Stepanov EA, Fedotov AB, Zheltikov AM. Multioctave, 3–18 μm sub-two-cycle supercontinua from self-compressing, self-focusing soliton transients in a solid. Opt Lett 2015;40:974–7.
[19] Mouawad O, Béjot P, Billard F, Mathey P, Kibler B, Désévédavy F, Gadret G, Jules JC, Faucher O, Smektala F. Filament-induced visible-to-mid-IR supercontinuum in a ZnSe crystal: Towards multi-octave supercontinuum absorption spectroscopy. Opt Mater 2016;60:355–8.
[20] Šuminas R, Tamošauskas G, Valiulis G, Jukna V, Couairon A, Dubietis A. Multi-octave spanning nonlinear interactions induced by femtosecond filamentation in polycrystalline ZnSe. Appl Phys Lett 2017;110:241106.
[21] Šuminas R, Marcinkevičiūtė A, Tamošauskas G, Dubietis A. Even and odd harmonics-enhanced supercontinuum generation in polyscrystalline zinc-blende semiconductors. J Opt Soc Am B 2019;36:A22–7.
[22] Werner K, Hastings MG, Schweinsberg A, Wilmer BL, Austin D, Wolfe CM, Kolesik M, Ensley TR, Vanderhoef L, Valenzuela A, Chowdhury E. Ultrafast mid-infrared high harmonic and supercontinuum generation with n_2 characterization in zinc selenide. Opt Express 2019;27:2867–85.
[23] Marcinkevičiūtė A, Jukna V, Šuminas R, Garejev N, Tamošauskas G, Dubietis A. Femtosecond filamentation and supercontinuum generation in bulk silicon. Opt Lett 2019;44:1343–6.
[24] Marcinkevičiūtė A, Tamošauskas G, Dubietis A. Supercontinuum generation in mixed thallous halides KRS-5 and KRS-6. Opt Mater 2018;78:339–44.
[25] Yang Y, Bi W, Li X, Liao M, Gao W, Ohishi Y, Fang Y, Li Y. Ultrabroadband supercontinuum generation through filamentation in lead fluoride crystal. J Opt Soc Am B 2019;36:A1–7.

[26] Weber MJ. Handbook of optical materials. London: CRC Press; 2003.
[27] Adair RL, Chase LL, Payne SA. Nonlinear refractive index of optical crystals. Phys Rev B 1989;39:3337–50.
[28] Sheik-Bahae M, Hutchings DC, Hagan DJ, Van Stryland EW. Dispersion of bound electronic nonlinear refraction in solids. IEEE J Quantum Electron 1991;27:1296–309.
[29] Kohl-Landgraf J, Nimsch JE, Wachtveitl J. LiF, an underestimated supercontinuum source in femtosecond transient absorption spectroscopy. Opt Express 2013;21:17060–5.
[30] Kuznetsov AV, Kompanets VO, Dormidonov AE, Chekalin SV, Shlenov SA, Kandidov VP. Periodic colour-centre structure formed under filamentation of mid-IR femtosecond laser radiation in a LiF crystal. Quantum Electron 2016;46:379–86.
[31] Chekalin SV, Kompanets VO, Dormidonov AE, Kandidov VP. Influence of induced colour centres on the frequency-angular spectrum of a light bullet of mid-IR radiation in lithium fluoride. Quantum Electron 2017;47:259–65.
[32] Chekalin SV, Kompanets VO, Dormidonov AE, Kandidov VP. Path length and spectrum of single-cycle mid-IR light bullets in transparent dielectrics. Quantum Electron 2018;48:372–7.
[33] Mao SS, Quéré F, Guizard S, Mao X, Russo RE, Petite G, Martin P. Dynamics of femtosecond laser interactions with dielectrics. Appl Phys A 2004;79:1695–709.
[34] Orlando S, Langford SC, Dickinson JT. Generation of color centers in alkali halide single crystals using ultrafast laser pulses. J Optoelecton Adv Mat 2010;12:707–10.
[35] Dickinson JT, Orlando S, Avanesyan SM, Langford SC. Color center formation in soda lime glass and NaCl single crystals with femtosecond laser pulses. Appl Phys A 2004;79:859–64.
[36] Dickinson JT, Langford SC, Avanesyan SM, Orlando S. Color center formation in KCl and KBr single crystals with femtosecond laser pulses. Appl Surf Sci 2007;253:7874–8.
[37] Couairon A, Brambilla E, Corti T, Majus D, de J. Ramírez-Góngora O, Kolesik M. Practitioner's guide to laser pulse propagation models and simulation. Eur Phys J Special Topics 2011;199:5–76.
[38] Dicaire I, Jukna V, Praz C, Milian C, Summerer L, Couairon A. Spaceborne laser filamentation for atmospheric remote sensing. Laser Photon Rev 2016;10:481–93.
[39] Bravy BG, Gordienko VM, Platonenko VT. Self-compression of terawatt level picosecond 10 μm laser pulses in NaCl. Laser Phys Lett 2014;11:065401.